Inorganic Chemistry
Article

Inorg. Chem. **2011**, *50*, 1733–1742 **1733**
DOI: 10.1021/ic102178d

Structural Principles of Semiconducting Group 14 Clathrate Frameworks

Antti J. Karttunen,*,† Thomas F. Fässler,‡ Mikko Linnolahti,† and Tapani A. Pakkanen†

†*Department of Chemistry, University of Eastern Finland, P.O. Box 111, FI-80101 Joensuu, Finland, and*
‡*Department of Chemistry, Technische Universität München, Lichtenbergstrasse 4, 85747 Garching, Germany*

Received October 29, 2010

We have performed a comprehensive theoretical investigation of the structural principles of semiconducting clathrate frameworks composed of the Group 14 elements carbon, silicon, germanium, and tin. We have investigated the basic clathrate frameworks, together with their polytypes, intergrowth clathrate frameworks, and extended frameworks based on larger icosahedral building blocks. Quantum chemical calculations with the PBE0 hybrid density functional method provided a clear overview of the structural trends and electronic properties among the various clathrate frameworks. In agreement with previous experimental and theoretical studies, the clathrate II framework proved to be the energetically most favorable, but novel hexagonal polytypes of clathrate II also proved to be energetically very favorable. In the case of silicon, several of the studied clathrate frameworks possess direct and wide band gaps. The band structure diagrams and simulated powder X-ray patterns of the studied frameworks are provided and systematic preliminary evaluation of guest-occupied frameworks is conducted to shed light on the characteristics of novel, experimentally feasible clathrate compositions.

Introduction

Semiconducting clathrates[1−3] are inorganic inclusion compounds that are structurally related to clathrate hydrates.[4] The semiconducting clathrates are currently investigated intensively, because of their high application potential as thermoelectric materials for converting temperature differences to electric energy (the Seebeck effect) or vice versa (the Peltier effect).[5,6] Semiconducting clathrates composed of Group 14 elements were discovered as prospective thermoelectric materials[7,8] soon after the introduction of the "Phonon Glass−Electron Crystal" (PGEC) concept.[9] The atomic structure of a PGEC material features cavities or tunnels occupied by heavy, "rattling" guest atoms, which produce a phonon damping effect, reducing the lattice thermal conductivity significantly. If, at the same time, the mobility of the charge carriers remains high, the structural motif opens the possibility of preparing materials with high thermoelectric efficiency. The three-dimensional microporous framework of the semiconducting clathrates is composed of fused atomic cages, which are normally occupied by guest atoms (see Figure 1). For semiconducting clathrates, where the framework is composed of Group 14 atoms, the most typical guest atoms in the cagelike cavities are alkali, alkaline-earth, and halogen atoms. The guest atoms are considered to transfer electrons to the framework (alkali/alkaline-earth guests) or vice versa (halogen guests), according to the Zintl concept.[1−3] To balance the charge of the framework, the structures usually include some heteroatoms, such as Group 13 or Group 15 atoms, in the framework.

Clathrate frameworks are classified into structure types labeled with roman numerals, based on the types of their constituent cages. The structural characteristics of the various basic clathrate frameworks have been summarized in an excellent review by Rogl.[10] The classification scheme used for semiconducting Group 14 clathrates was originally devised for the clathrate hydrates, for which the structure types I−VII have been observed (I−III, VI, VII) or proposed (IV, V).[10,11] Furthermore, an additional hexagonal structure type (H) is known for the clathrate hydrates.[12] The first

*To whom correspondence should be addressed. E-mail: antti.j.karttunen@iki.fi.

(1) Kovnir, K. A.; Shevelkov, A. V. *Russ. Chem. Rev.* **2004**, *73*, 923–938.
(2) Beekman, M.; Nolas, G. S. *J. Mater. Chem.* **2008**, *18*, 842–851.
(3) Christensen, M.; Johnsen, S.; Iversen, B. B. *Dalton Trans.* **2010**, *39*, 978–992.
(4) Jeffrey, G. A. *J. Inclusion Phenom.* **1984**, *1*, 211–222.
(5) Rowe, D. M. In *CRC Thermoelectrics Handbook*; Rowe, D. M., Ed.; Taylor & Francis Group, LLC: Boca Raton, FL, 2006; Chapter 1.
(6) Sootsman, J. R.; Chung, D. Y.; Kanatzidis, M. G. *Angew. Chem., Int. Ed.* **2009**, *48*, 8616–8639.
(7) Nolas, G. S.; Cohn, J. L.; Slack, G. A.; Schujman, S. B. *Appl. Phys. Lett.* **1998**, *73*, 178–180.
(8) Blake, N. P.; Møllnitz, L.; Kresse, G.; Metiu, H. *J. Chem. Phys.* **1999**, *111*, 3133–3144.
(9) Slack, G. A. In *CRC Handbook of Thermoelectrics*; Rowe, D. M., Ed.; CRC Press: Boca Raton, FL, 1995; p 407.
(10) Rogl, P. *Thermoelectrics Handbook: Macro to Nano*; Rowe, D. M., Ed.; CRC Press: Boca Raton, FL, 2006; Chapter 32.
(11) Kosyakov, V. I.; Solodovnikov, S. F.; Shestakov, V. A. *J. Struct. Chem.* **1996**, *37*, 986–989.
(12) Udachin, K. A.; Ratcliffe, C. I.; Enright, G. D.; Ripmeester, J. A. *Supramol. Chem.* **1997**, *8*, 173–176.
(13) Kasper, J. S.; Hagenmuller, P.; Pouchard, M.; Cros, C. *Science* **1965**, *150*, 1713–1714.

Published on Web 12/28/2010

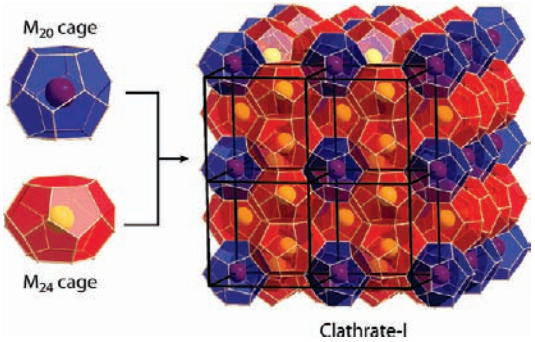

Figure 1. General structural motif of the Group 14 semiconducting clathrates. The clathrate illustrated here is composed of fused 20- and 24-membered atomic cages filled with guest atoms. Unit-cell edges are drawn in black color.

semiconducting Group 14 clathrates, belonging to the structure types I and II, were originally discovered in the 1960s.[13] Later, semiconducting Group 14 clathrates[1] also have been prepared for the structure types III,[14] VIII,[15] and IX.[16] Hence, so far, the basic frameworks IV−VII and H have not been observed for semiconducting Group 14 clathrates. However, a different type of intermetallic representative of structure type IV has been recently prepared.[17] Furthermore, a completely new clathrate structure type *oP*60 has been synthetized very recently in the form of BaGe5.[18]

In addition to the guest-occupied clathrate frameworks, almost empty Si and Ge clathrates of structure type II also are known.[19] The "guest-free" clathrate frameworks are of particular interest, because they could turn out to be very useful materials for optoelectronics or photovoltaics.[19b,20] Furthermore, the guest-free clathrate frameworks are also interesting, because of their fundamental role as new allotropes of silicon and germanium.

Several theoretical studies on the structural characteristics and relative stabilities of various clathrate frameworks have been conducted to provide helpful information for researchers working toward the synthesis of novel semiconducting clathrates. Here, we provide a short summary of the studies, where the main emphasis has been on the structural comparisons between different clathrate frameworks. Empty clathrate frameworks of Type I and Type II have been theoretically investigated in various studies for carbon,[21] silicon,[22] germanium,[23] and tin.[24] Starting from the fact that several clathrate frameworks are actually duals of the intermetallic Frank−Kasper phases, O'Keeffe et al. studied the basic frameworks I−IV and various extended intergrowth frameworks for C, Si, and Ge.[25,26] A set of basic clathrate frameworks was also investigated for all Group 14 elements by Rousseau et al., to shed light on the structural characteristics of metal-doped clathrate compounds.[27] Several clathrate frameworks were also investigated by Conesa in a study on various low-density allotropes of silicon and germanium.[28] Another recent survey of low-density allotropy in silicon included a larger set of basic clathrate frameworks, as well as the extended intergrowth frameworks suggested by O'Keeffe et al.[29] Finally, Benedek et al. investigated three structural series of hollow carbon structures, where the first members of the series are the basic clathrate frameworks I, II, and IV.[30] Interestingly, the hollow carbon structures are very closely related to the recently investigated icosahedral diamondoids and diamondoid analogues of heavier Group 14 elements silicon, germanium, and tin.[31] Introducing larger icosahedral building blocks to the clathrate frameworks seems to be a promising way to create modifications where the density is somewhere between that of a basic clathrate framework and that of the dense diamond-like elemental form.

So far, the majority of the experimental and theoretical work on semiconducting Group 14 clathrates has focused on structures of Type I and Type II. Therefore, systematic investigation of the other basic clathrate frameworks and more-complex extended frameworks presents considerable possibilities for the realization of novel materials for thermoelectric and optoelectronic applications. Here, we perform a systematic quantum chemical study on the various clathrate frameworks of the Group 14 elements carbon, silicon, germanium, and tin. In addition to the basic clathrate frameworks I−IX and H, we study complex intergrowth clathrates and extended clathrate frameworks based on larger icosahedral building blocks. The structural characteristics, stabilities, and electronic properties of the low-density allotropes of the elements are investigated, and the various aspects related to the experimental preparation of Group 14 clathrates also are considered.

(14) Bobev, S.; Sevov, S. C. *J. Am. Chem. Soc.* **2001**, *123*, 3389–3390.
(15) Eisenmann, B.; Schäfer, H.; Zagler, R. *J. Less-Common. Met.* **1986**, *118*, 43–55.
(16) (a) Kroener, R.; Nesper, R.; von Schnering, H. G. *Z. Kristallogr.* **1988**, *182*, 164–165. (b) von Schnering, H. G.; Kröner, R.; Carrillo-Cabrera, W.; Peters, K.; Nesper, R. *Z. Kristallogr.—New Cryst. Struct.* **1998**, *213*, 665–666.
(17) Lin, Q.; Corbett, J. D. *Inorg. Chem.* **2008**, *47*, 10825–10831.
(18) Aydemir, U.; Akselrud, L.; Carrillo-Cabrera, W.; Candolfi, C.; Oeschler, N.; Baitinger, M.; Steglich, F.; Grin, Y. *J. Am. Chem. Soc.* **2010**, *132*, 10984–10985.
(19) (a) Gryko, J.; McMillan, P. F.; Marzke, R. F.; Ramachandran, G. K.; Patton, D.; Deb, S. K.; Sankey, O. F. *Phys. Rev. B* **2000**, *62*, R7707–R7710. (b) Ammar, A.; Cros, C.; Pouchard, M.; Jaussaud, N.; Bassat, J.-M.; Villeneuve, G.; Duttine, M.; Ménétrier, M.; Reny, E. *Solid State Sci.* **2004**, *6*, 393–400. (c) Guloy, A. M.; Ramlau, R.; Tang, Z.; Schnelle, W.; Baitinger, M.; Grin, Y. *Nature* **2006**, *443*, 320–323.
(20) Fässler, T. F. *Angew. Chem., Int. Ed.* **2007**, *46*, 2572–2575.
(21) Nesper, R.; Vogel, K.; Blöchl, P. E. *Angew. Chem., Int. Ed. Engl.* **1993**, *32*, 701–703.
(22) Adams, G. B.; O'Keeffe, M.; Demkov, A. A.; Sankey, O. F.; Huang, Y.-M. *Phys. Rev. B* **1994**, *49*, 8048–8053.
(23) Dong, J.; Sankey, O. F. *J. Phys.: Condens. Matter* **1999**, *11*, 6129–6145.
(24) Myles, C. W.; Dong, J.; Sankey, O. F. *Phys. Rev. B* **2001**, *64*, 165202.
(25) O'Keeffe, M.; Adams, G. B.; Sankey, O. F. *Philos. Mag. Lett.* **1998**, *78*, 21–28.
(26) The basic clathrate structure Types III and IV are interchanged in ref 25.
(27) Ker, A.; Todorov, E.; Rousseau, R.; Uehara, K.; Lannuzel, F.-X.; Tse, J. S. *Chem.—Eur. J.* **2002**, *8*, 2787–2797.
(28) Conesa, J. C. *J. Phys. Chem. B* **2002**, *106*, 3402–3409.
(29) Zwijnenburg, M. A; Jelfs, K. E.; Bromley, S. T. *Phys. Chem. Chem. Phys.* **2010**, *12*, 8505–8511.
(30) Benedek, G.; Galvani, E.; Sanguinetti, S.; Serra, S. *Chem. Phys. Lett.* **1995**, *244*, 339–344.
(31) (a) Linnolahti, M.; Karttunen, A. J.; Pakkanen, T. A. *J. Phys. Chem. C* **2007**, *111*, 18118–18126. (b) Karttunen, A. J.; Linnolahti, M.; Pakkanen, T. A. *J. Phys. Chem. C* **2008**, *112*, 16324–16330.
(32) (a) Perdew, J. P.; Burke, K.; Ernzerhof, M. *Phys. Rev. Lett.* **1996**, *77*, 3865–3868. (b) Adamo, C.; Barone, V. *J. Chem. Phys.* **1999**, *110*, 6158–6170.
(33) (a) Dovesi, R.; Saunders, V. R.; Roetti, C.; Orlando, R.; Zicovich-Wilson, C. M.; Pascale, F.; Civalleri, B.; Doll, K.; Harrison, N. M.; Bush, I. J.; D'Arco, Ph.; Llunell, M. *CRYSTAL06 User's Manual*; University of Torino: Torino, Italy, 2006. (b) Dovesi, R.; Saunders, V. R.; Roetti, R.; Orlando, R.; Zicovich-Wilson, C. M.; Pascale, F.; Civalleri, B.; Doll, K.; Harrison, N. M.; Bush, I. J.; D'Arco, P.; Llunell, M.; *CRYSTAL09 User's Manual*: University of Torino: Torino, Italy, 2009. (c) Dovesi, R.; Orlando, R.; Civalleri, B.; Roetti, R.; Saunders, V. R.; Zicovich-Wilson, C. M. *Z. Kristallogr.* **2005**, *220*, 571–573.

Computational Details

The clathrate structures were investigated using the PBE0 hybrid density functional[32] and localized atomic basis sets composed of Gaussian-type functions. All calculations were performed using the CRYSTAL06 and CRYSTAL09 software packages.[33] In periodic calculations, the choice of the Gaussian-type localized atomic basis set requires careful consideration. Basis sets originally developed for molecular calculations contain diffuse basis functions to model the tails of wave function; however, in periodic calculations, where the entire space is filled with basis functions, such diffuse functions are usually unnecessary and lead to numerical difficulties and/or a severe degradation of performance.[34] The following split-valence + polarization (SVP) basis sets were applied for the studied systems: carbon: a modified all-electron 6-21G* basis set;[35] silicon: a modified all-electron def2-SVP basis set;[36] germanium: a SVP basis set derived from the molecular cc-pVDZ-PP and def2-SVP basis sets, together with a 10-electron scalar-relativistic pseudopotential for the 1s 2s 2p core;[37,38] tin: a SVP basis set derived from the molecular def2-SVP basis set, together with a 28-electron scalar-relativistic pseudopotential for the 1s 2s 2p 3s 3p 3d core.[38] Further basis set details can be found in the Supporting Information. Comparison with experimental lattice parameters and bulk moduli for the diamond-like α-structures showed that the results obtained at the PBE0/SVP level of theory were in good agreement with the experiment and state-of-the-art DFT calculations based on projector augmented waves[39] (relative errors for the predicted lattice parameters were 0.1%−1.1%, in comparison to the experiment; see the Supporting Information for details). In structural optimizations, both the cell parameters and the atomic positions of the studied systems were allowed to relax within the constraints imposed by the space group symmetry. The shrinking factors (SHRINK) used for generating a Monkhorst−Pack-type[40] grid of *k*-points in the reciprocal space are listed in the Supporting Information. Calibration calculations confirmed the applied *k*-point grids to yield well-converged results. For the evaluation of the Coulomb and exchange integrals (TOLINTEG), tight tolerance factors of 8, 8, 8, 8, and 16 were used. Default optimization convergence thresholds and an extra large integration grid (XLGRID) for the density-functional part were applied in the calculations. Harmonic vibrational frequency calculations were performed to confirm all studied clathrate frameworks as true local minima (for very large structures, such as the I+II intergrowth clathrate with 920 atoms in the unit cell, the frequency calculations could only be performed for carbon and only with the computationally less demanding pure PBE density functional). The vibrational frequencies were obtained using the computational scheme implemented in CRYSTAL.[41]

Results and Discussion

1. Basic clathrate frameworks. The structural characteristics of the studied Group 14 clathrate frameworks are summarized in Table 1. In the case of the basic and intergrowth frameworks, the data in the table has mostly been derived from the review of Rogl.[10] For several clathrate structure types, there exists a densely packed intermetallic dual structure, where the atomic positions in the intermetallic structure correspond to the cage centers in the clathrate structures. For the structures that are also included in the Reticular Chemistry Structure Resource (RCSR) database of crystal nets,[42] we have listed the RCSR code to facilitate the usage of the database. In addition to the frameworks included in Table 1, we investigated several other hypothetical clathrate-like frameworks found in the RCSR database (structure codes: mds, odf, odg, odh, odi, odj, odk, odl, odm). However, because of their relatively strained nature, they are not discussed in detail here (the data for these additional structures can be found in the Supporting Information).

The structures of the basic clathrate frameworks I−IX and H, together with their constituent cages, are illustrated in Figure 2. An interesting structural relationship exists between the basic clathrate frameworks II (dual of Laves-phase[43] $MgCu_2$) and V (dual of Laves-phase $MgZn_2$), which are both composed of $[5^{12}]$ and $[5^{12}6^4]$ cages. In clathrate II, the arrangement of the larger $[5^{12}6^4]$ cages is similar to that of carbon atoms in the diamond lattice, whereas in clathrate V, the $[5^{12}6^4]$ cages are arranged like the carbon atoms in lonsdaleite (that is, hexagonal diamond). Using the Ramsdell notation for the packing of the $[5^{12}6^4]$ cages, clathrates II and V are the 3C and 2H polytypes, respectively. To shed more light on the polytypism of the clathrate framework, we derived one more additional "basic" clathrate framework: a 4H polytype of clathrate II (see Figure 2). The hypothetical structure is the dual of Laves-phase $MgNi_2$. Further polytypes such as 6H can be derived in an analogous way. The polytypism of the Group 14 clathrate frameworks is an interesting example of the rather common polytypism of the Group 14 elements. Another recent example of Group 14 polytypism is the study on structure and electronic properties of the 4H modification of germanium.[44]

The relative energies, band gaps, and densities of the basic clathrate frameworks for all studied Group 14 elements are listed in Table 2 and illustrated in Figure 3. The relative energies of the structurally optimized clathrate structures are given, with respect to the diamond-like α-structures of the respective elements. For all elements, the clathrate framework II turned out to be the most stable one with respect to the α-structure, in agreement with previous studies on clathrate frameworks, which have included structure type II.[21−29] However, the hexagonal polytypes of the cubic clathrate II—that is, 2H−II (clathrate V) and 4H−II—lie energetically very close to the 3C−II polytype, suggesting the possibility of "clathrate II polytypism". Furthermore, the energy differences between the most stable clathrate framework II and some other basic clathrate frameworks are also quite small. For example, in the case of silicon, structure types I, III, IV, VIII, and H are only 0.02−0.04 eV/atom less stable than

(34) Kudin, K.; Scuseria, G. E. *Phys. Rev. B* **2000**, *61*, 16440–16453.
(35) Catti, M.; Pavese, A.; Dovesi, R.; Saunders, V. R. *Phys. Rev. B* **1993**, *47*, 9189–9198.
(36) (a) Schaefer, A.; Horn, H.; Ahlrichs, R. *J. Chem. Phys.* **1992**, *97*, 2571–2577. (b) Weigend, F.; Ahlrichs, R. *Phys. Chem. Chem. Phys.* **2005**, *7*, 3297–3305.
(37) Peterson, K. A. *J. Chem. Phys.* **2003**, *119*, 11099–11112.
(38) Metz, B.; Stoll, H.; Dolg, M. *J. Chem. Phys.* **2000**, *113*, 2563–2569.
(39) Hummer, K.; Harl, J.; Kresse, G. *Phys. Rev. B* **2009**, *80*, 115205.
(40) Monkhorst, H. J.; Pack, J. D. *Phys. Rev. B* **1976**, *13*, 5188–5192.
(41) (a) Pascale, F.; Zicovich-Wilson, C. M.; Lopez, F.; Civalleri, B.; Orlando, R.; Dovesi, R. *J. Comput. Chem.* **2004**, *25*, 888–897. (b) Zicovich-Wilson, C. M.; Pascale, F.; Roetti, C.; Saunders, V. R.; Orlando, R.; Dovesi, R. *J. Comput. Chem.* **2004**, *25*, 1873–1881.
(42) O'Keeffe, M.; Peskov, M. A.; Ramsden, S. J.; Yaghi, O. M. *Acc. Chem. Res.* **2008**, *41*, 1782−1789 (http://rcsr.anu.edu.au).
(43) Stein, F.; Palm, M.; Sauthoff, G. *Intermetallics* **2004**, *12*, 713–720.
(44) Kiefer, F.; Hlukhyy, V.; Karttunen, A. J.; Fässler, T. F.; Gold, C.; Scheid, E.-W.; Scherer, W.; Nylén, J.; Häussermann, U. *J. Mater. Chem.* **2010**, *20*, 1780–1786.

Table 1. Summary of the Studied Group 14 Clathrate Frameworks

clathrate	space group	atoms/cell[a]	building blocks[b]	dual structure[c]	RCSR ID[d]
			Basic Frameworks		
I	$Pm\bar{3}n$ (223)	46	$[5^{12}]_2[5^{12}6^2]_6$	Cr_3Si	mep
II	$Fd\bar{3}m$ (227)	136	$[5^{12}]_{16}[5^{12}6^4]_8$	$MgCu_2$	mtn
III	$P4_2/mnm$ (136)	172	$[5^{12}]_{10}[5^{12}6^2]_{16}[5^{12}6^3]_4$	Cr_6Fe_7	sig
IV[e]	$P6/mmm$ (191)	40	$[5^{12}]_3[5^{12}6^2]_2[5^{12}6^3]_2$	Zr_4Al_3	zra−d
V	$P6_3/mmc$ (194)	68	$[5^{12}]_8[5^{12}6^4]_4$	$MgZn_2$	mgz−x−d
VI	$I\bar{4}3d$ (220)	156	$[4^35^96^27^3]_{16}[4^45^4]_{12}$		
VII	$Im\bar{3}\bar{m}$ (229)	12	$[4^66^8]_2$		sod
VIII[f]	$I\bar{4}3m$ (217)	46	$[3^34^35^9]_6[3^34^35^9]_8$		
IX[g]	$P4_132$ (213)	100	$[5^{12}]_8$ + others		
H	$P6/mmm$ (191)	34	$[5^{12}]_3[4^35^66^3]_2[5^{12}6^8]_1$		doh
"II−4H"	$P6_3/mmc$ (194)	136	$[5^{12}]_{16}[5^{12}6^4]_8$	$MgNi_2$	
			Intergrowth Frameworks[25]		
I+II[h]	$Pm\bar{3}n$ (223)	920	$[5^{12}]_{98}[5^{12}6^2]_{18}[5^{12}6^4]_{46}$		tep
I+IV = III	$P4_2/mnm$ (136)	172	$[5^{12}]_{10}[5^{12}6^2]_{16}[5^{12}6^3]_4$	σ-Cr_6Fe_7	sig
II+IV−*a*	$Im\bar{3}$ (204)	460	$[5^{12}]_{98}[5^{12}6^2]_{12}[5^{12}6^3]_{12}[5^{12}6^4]_{40}$	$Mg_{32}(Al,Zn)_{49}$	tei
II+IV−*b*	$R\bar{3}m$ (166)	74	$[5^{12}]_{21}[5^{12}6^2]_6[5^{12}6^3]_6[5^{12}6^4]_6$	μ-W_6Fe_7	mur
			Extended Frameworks Based on Larger Icosahedral Building Blocks (I_h-Clathrates)[i]		
I−100	$Pm\bar{3}n$ (223)	230	$[5^{12}]_2[5^{12}6^2]_6[6^26_b^5]_6[5^26_b^5]_{48}$		
I−280	$Pm\bar{3}n$ (223)	644	$[5^{12}]_2[5^{12}6^2]_6[6^26_b^5]_{12}[5^26_b^5]_{96}$		
II−100	$Fd\bar{3}m$ (227)	680	$[5^{12}]_{16}[5^{12}6^4]_8[6^26_b^5]_{16}[5^26_b^5]_{144}$		
II−280	$Fd\bar{3}m$ (227)	1904	$[5^{12}]_{16}[5^{12}6^4]_8[6^26_b^5]_{32}[5^26_b^5]_{288}$		
IV−100	$P6/mmm$ (191)	200	$[5^{12}]_3[5^{12}6^2]_2[5^{12}6^3]_2[6^26_b^5]_5[5^26_b^5]_{36}$		
IV−280	$P6/mmm$ (191)	560	$[5^{12}]_3[5^{12}6^2]_2[5^{12}6^3]_2[6^26_b^5]_{10}[5^26_b^5]_{72}$		

[a] Number of framework atoms in the crystallographic unit cell. [b] The atomic cages the framework is composed of (cf. Figure 1). Notation: $[5^{12}6^2]$ = a cage with 12 five-membered rings and 2 six-membered rings. [c] The intermetallic dual structure of the clathrate framework.[10,25] [d] Symbol for the framework in the Reticular Chemistry Structure Resource database of crystal nets.[42] [e] A unit cell with 40 atoms was used instead of the ideal 80 atoms suggested for clathrate hydrates.[4,10,45] [f] The small $[3^34^3]$ voids (8-vertex cavities) are often left of out the framework description.[1] [g] Some of the cages are not well-defined and the framework contains 32 three-coordinated atoms. Hence, the IX framework was investigated as $Si_{68}P_{32}$. [h] The dual structure of a hypothetical primitive cubic derivative of $Mg_{32}(Al,Zn)_{49}$ (cf. II+IV−a).[25] [i] The 6b-rings are not planar, but the ring is in a boat conformation (cf. Figure 4). The 280-I_h-clathrates contain additional small voids with 12 vertices.

the clathrate II framework. The basic frameworks VI and VII containing a large number of four-membered rings are very strained in comparison to the other frameworks. Interestingly, the structure of clathrate H also includes four-membered rings; however, despite this, the framework is not very strained. The same issue was also discussed by Bromley et al.[29]

A detailed look at the structural characteristics of the polyhedral constituent cages helps to understand the relative stabilities of the clathrate frameworks. We extracted the polyhedral constituent cages from their parent clathrate structures, saturated them with hydrogen atoms, and optimized the resulting cage structures at the PBE0/SVP level of theory (the relative energies of the cages are shown in Table S4 and Figure S3 in the Supporting Information). In summary, the relative stabilities of the clathrate frameworks are directly related to the strain energies of their constituent cages. The dodecahedral $[5^{12}]$ cage proved to be the least-strained cage for all elements. The cage contains only five-membered rings and the bond angles are very close to the optimal 109.5°. The $[5^{12}6^2]$, $[5^{12}6^3]$, and $[5^{12}6^4]$ are slightly more strained than the $[5^{12}]$ cage, because of the planar six-membered rings, while the cages containing four-membered rings are noticeably more strained, particularly in the case of carbon. Generally, the polyhedral cages become less strained when moving from carbon down to tin, which is also true for the clathrate frameworks. In the energetically most favorable clathrate frameworks II, V, and 4H−II, the dominant building block is the least-strained $[5^{12}]$ cage, with their ratio to the slightly more-strained $[5^{12}6^4]$ cages being 2:1. The basic frameworks I, III, and IV contain $[5^{12}]$, $[5^{12}6^2]$, and $[5^{12}6^3]$ cages, making them only slightly less favorable, in comparison to the most favorable clathrate frameworks II, V, and 4H−II. In the case of clathrate framework H, the higher ratio of $[5^{12}]$ cages, in relation to the $[4^35^66^3]$ cages containing four-membered rings (3:2), makes the framework energetically still quite favorable, despite the presence of the four-membered rings. In clathrate VIII, the structural distortion of the $[5^{12}]$ cages into the $[3^34^35^9]$ cages increases the structural strain of the framework. The basic frameworks VI and VII, which contain a large number of four-membered rings and no $[5^{12}]$ cages at all, are the most-strained ones. Similar reasoning helps to understand the relative stabilities of the intergrowth and I_h-clathrates that are discussed in the next sections. However, because of the much more complex structural characteristics of the intergrowth and I_h-clathrates, the polyhedral cages can become very distorted, in comparison to their ideal shapes, decreasing the relative stability of the clathrate framework significantly.

Basic clathrate framework IX is a special case, because, in addition to the normal four-coordinated atoms, it contains three-coordinated atoms. We investigated framework IX for one binary composition, $Si_{68}P_{32}$, substituting all three-coordinated atoms sites with phosphorus. Because of the binary composition, comparing the relative stability of the framework to that of the other frameworks is not feasible; however, the band gap and the density

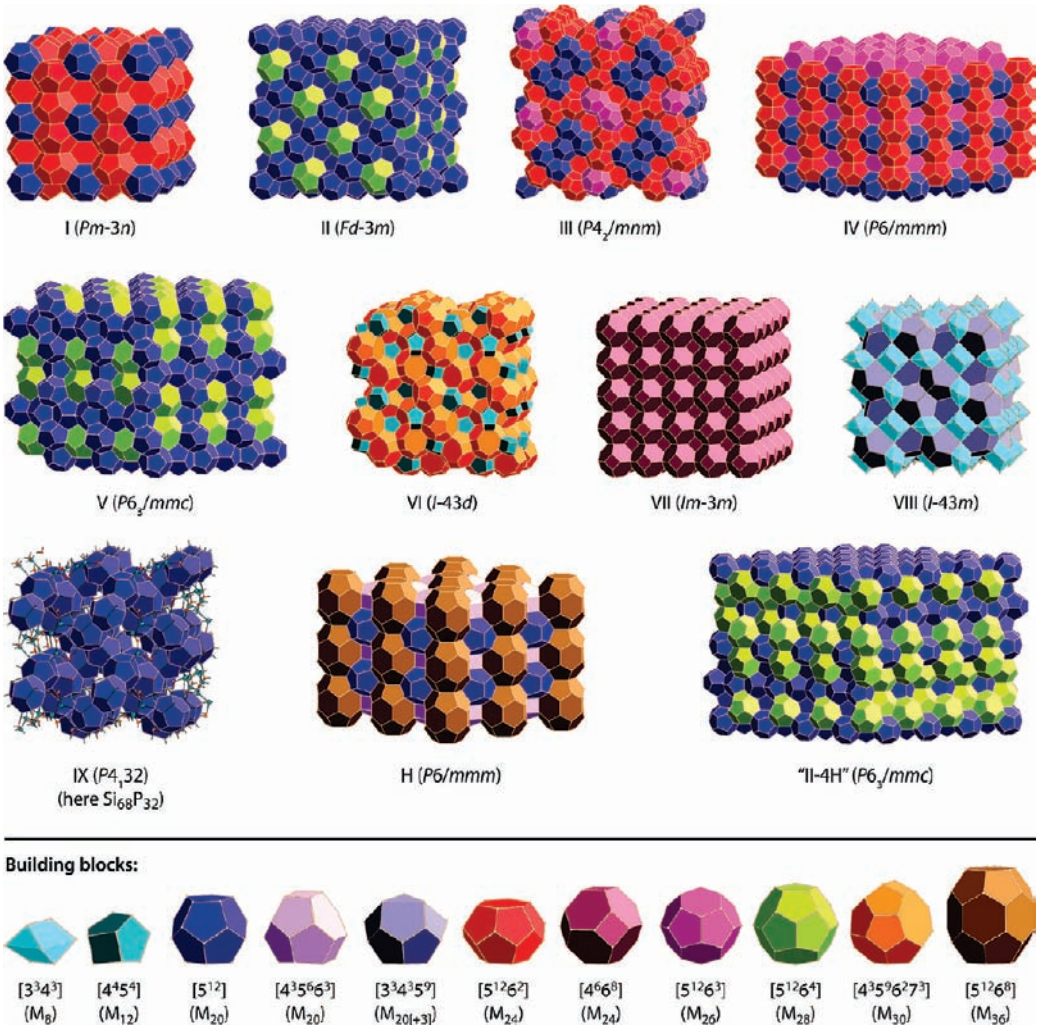

Figure 2. Studied basic clathrate frameworks.

calculated for the framework are consistent with those of the pure silicon clathrate frameworks. More-detailed studies on analogous Groups 14 and 15 binary IX frameworks, such as $Ge_{68}As_{32}$ or $Sn_{68}Sb_{32}$, could reveal new low-density structures with interesting properties. The analogous binary compositions could also be investigated for the very recently synthesized BaGe5 clathrate (*oP*60) containing three-coordinated atoms in the framework.[18]

Framework VI is the lowest-density structure among the basic clathrate frameworks for all elements, followed by the sodalite-like framework VII. In turn, the densest basic framework is clathrate VIII, which is composed of distorted pentagonal dodecahedra (20 + 3 atoms) and additional eight-vertex cavities. Note that, despite the notation $[3^34^35^9]_8$ used for the 20 + 3 polyhedra,[10] framework VIII does not contain any actual three- or four-membered rings.

Typical for microporous semiconductors, the band gaps of the studied basic clathrate frameworks are larger than the band gaps of the dense diamond structures.[21−29] The PBE0 method overestimates the indirect band gap of α-Si (theoretical gap = 1.9 eV, experimental gap at 0 K = 1.17 eV), while the band gaps calculated for the α-carbon (5.9 eV) and α-germanium (0.8 eV) are more similar to the experimental values (C, 5.4 eV; Ge, 0.74 eV).[46] α-Tin is correctly described as a zero-band-gap semiconductor, but the porous clathrate modifications of tin are semiconducting, with the exception of clathrate VII (zero band gap). For other elements, the strained clathrate VII structure also possesses a smaller band gap, in comparison to the dense diamond structures. Band structure diagrams and simulated powder X-ray patterns of the studied basic clathrate frameworks composed of silicon can be found in the Supporting Information (sections 2.1 and 2.3). Several silicon clathrates possess direct band gaps, namely, frameworks I, III, V, VII, H, II−4H, and IX. Interestingly, while the basic framework II is not a direct-band-gap semiconductor for silicon, both hexagonal modifications of the same framework, clathrates V and II−4H, possess direct band gaps.

2. Intergrowth Clathrate Frameworks. The intergrowth clathrate frameworks were derived from the basic clathrate frameworks by O'Keeffe et al.,[25] based on the fact that several clathrate frameworks are actually duals of the tetrahedrally close-packed intermetallic structures also

(45) O'Keeffe, M.; Hyde, B. G. *Crystal Structures I: Patterns and Symmetry*; Mineral Society of America: Washington, DC, 1996.

(46) Kittel, C. *Introduction to Solid State Physics*, 8th Ed.; John Wiley & Sons: Hoboken, NJ, 2005; p 190.

Table 2. Relative Energies (ΔE), Band Gaps, and Densities of the Studied Group 14 Clathrate Frameworks

	Relative Energy, ΔE (eV/atom)[a]				Band Gap (eV)				Density (g/cm^3)			
structure	C	Si	Ge	Sn	C	Si	Ge	Sn	C	Si	Ge	Sn
α (diamond)	0.0	0.0	0.0	0.0	5.9	1.9	0.8	0.0	3.52	2.29	5.26	5.63
Basic Frameworks												
I	0.15	0.10	0.05	0.04	6.2	2.8	2.4	1.8	3.08	2.00	4.66	5.02
II	0.11	0.08	0.04	0.03	6.0	2.8	1.9	1.4	3.06	1.98	4.61	4.96
III	0.15	0.10	0.06	0.04	6.1	2.7	2.2	1.6	3.07	2.00	4.64	4.99
IV	0.17	0.12	0.07	0.05	6.1	2.7	2.0	1.4	3.05	1.99	4.61	4.97
V	0.12	0.09	0.04	0.03	6.0	2.8	1.9	1.4	3.05	1.98	4.61	4.96
VI	0.48	0.25	0.19	0.14	6.6	2.8	2.2	1.6	2.78	1.80	4.14	4.45
VII	0.47	0.30	0.24	0.18	5.6	1.7	0.7	0.0	2.87	1.83	4.19	4.50
VIII	0.26	0.11	0.09	0.07	7.3	2.9	2.1	1.5	3.20	2.08	4.80	5.15
IX[b]						2.8				1.99		
H	0.18	0.12	0.07	0.05	5.6	2.6	1.7	1.2	3.00	1.94	4.50	4.83
II-4H	0.12	0.09	0.04	0.03	6.0	2.8	1.9	1.4	3.05	1.98	4.61	4.96
Intergrowth Frameworks												
I+II	0.37				4.7				3.03			
I+IV=III	0.15	0.10	0.06	0.04	6.1	2.7	2.2	1.6	3.07	2.00	4.64	4.99
II+IV−*a*	0.20	0.13	0.08	0.06	5.9	2.6	1.5	1.0	3.04	1.98	4.60	4.96
II+IV−*b*	0.15	0.10	0.06	0.04	6.0	2.7	2.0	1.5	3.05	1.98	4.61	4.96
Extended Frameworks Based on Larger Icosahedral Building Blocks (I_h-Clathrates)												
I−100	0.24	0.11	0.09	0.07	6.7	1.9	1.2	1.0	3.33	2.19	5.03	5.42
I−280	0.27	0.12	0.11		5.6	1.7	0.9		3.39	2.24	5.13	
II−100	0.19	0.10	0.08	0.06	6.9	1.9	1.3	0.7	3.30	2.17	4.97	5.36
II−280	0.21	0.11	0.09	0.08	6.3	1.6	0.6	0.1	3.37	2.22	5.07	5.46
IV−100	0.24	0.14	0.10	0.08	6.8	1.6	1.0	0.6	3.30	2.17	4.98	5.37
IV−280		0.14	0.12			1.3	0.6			2.22	5.07	

[a] Energy relative to the diamond-like α-structure. [b] Only the binary $Si_{68}P_{32}$ structure was investigated in the case of the IX framework.

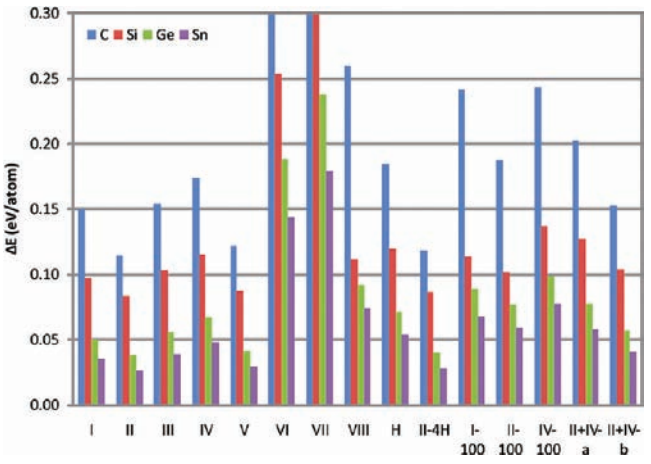

Figure 3. Relative energies of the studied clathrate modifications (given in units of eV/atom, with respect to the diamond-like α-structure).

known as Frank−Kasper structures. The intergrowth clathrates and their structural principles are illustrated in Figure 4. The most-complex intergrowth clathrate described by O'Keeffe et al. is the intergrowth of basic frameworks II and IV.[26] The structure, labeled here as II+IV−*a*, contains 460 atoms per unit cell and it is the dual of the intermetallic Bergman phase $Mg_{32}(Al,Zn)_{49}$. O'Keeffe et al. also derived another complex framework, which is the dual structure of a hypothetical primitive cubic derivative of the Bergman phase. This intergrowth structure has 920 atoms in the unit cell, and it can be considered to be the intergrowth of basic clathrate frameworks I and II. The other intergrowth described structures are simpler, with the intergrowth of frameworks I and IV being, in fact, identical to framework III (for clarity, we have nevertheless classified framework III to be a "basic" framework). For the intergrowth of basic frameworks II and IV, the simplest structure, labeled here as II+IV−*b*, contains 74 atoms in the rhombohedral unit cell (RCSR: mur). In addition to the rhombohedral intergrowth, we also investigated the hexagonal (2H) polytype of the II+IV intergrowth described by O'Keeffe et al. (RCSR: muh). The hexagonal intergrowth turned out to be practically isoenergetic with the rhombohedral one; therefore, in the following, we only discuss the rhombohedral variant.

The relative energies, band gaps, and densities of the intergrowth clathrate frameworks for all studied Group 14 elements are listed in Table 2 and are illustrated in Figure 3. Because of software-imposed limits for the number of basis functions per cell, the I+II intergrowth clathrate (920 atoms in the unit cell) could only be investigated for carbon. In agreement with previous results,[25] the structure turned out to be one of the most strained frameworks. However, the I+II carbon clathrate is not representative for the other Group 14 elements, since hybridization with spatially more-diffuse *d*-orbitals is not available for bonding. The intergrowth clathrates II+IV−*a* and II+IV−*b* are more interesting, because they show reasonably low relative energies. In fact, the rhombohedral II+IV−*b* structure is one of the least-strained frameworks for all elements. As can be expected, based on their structural relationships, the densities of the intergrowth frameworks are very similar to the densities of their parent frameworks. Interestingly, possible intergrowth structures of the extended clathrate frameworks, based on

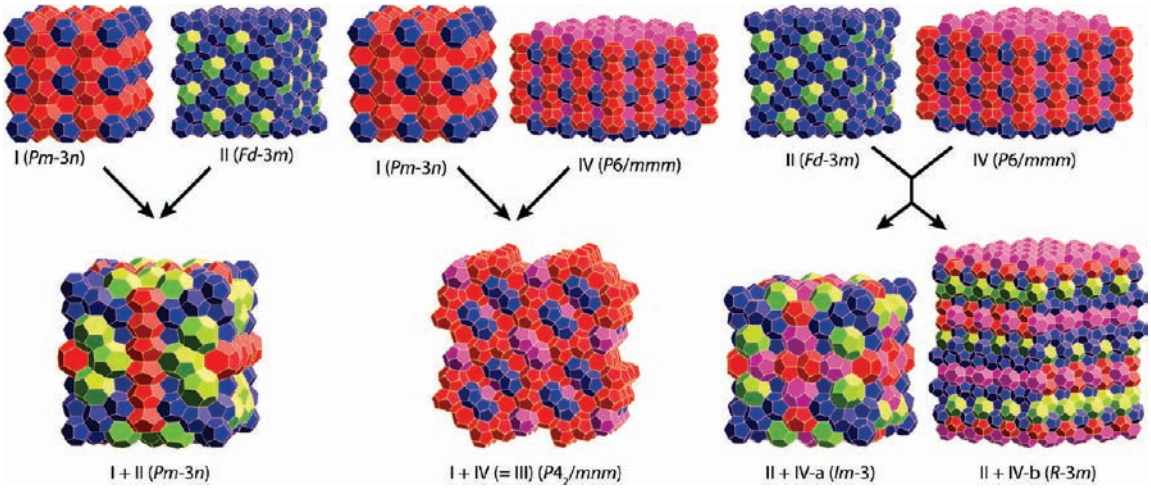

Figure 4. Structural principles of the studied intergrowth clathrate frameworks.[25]

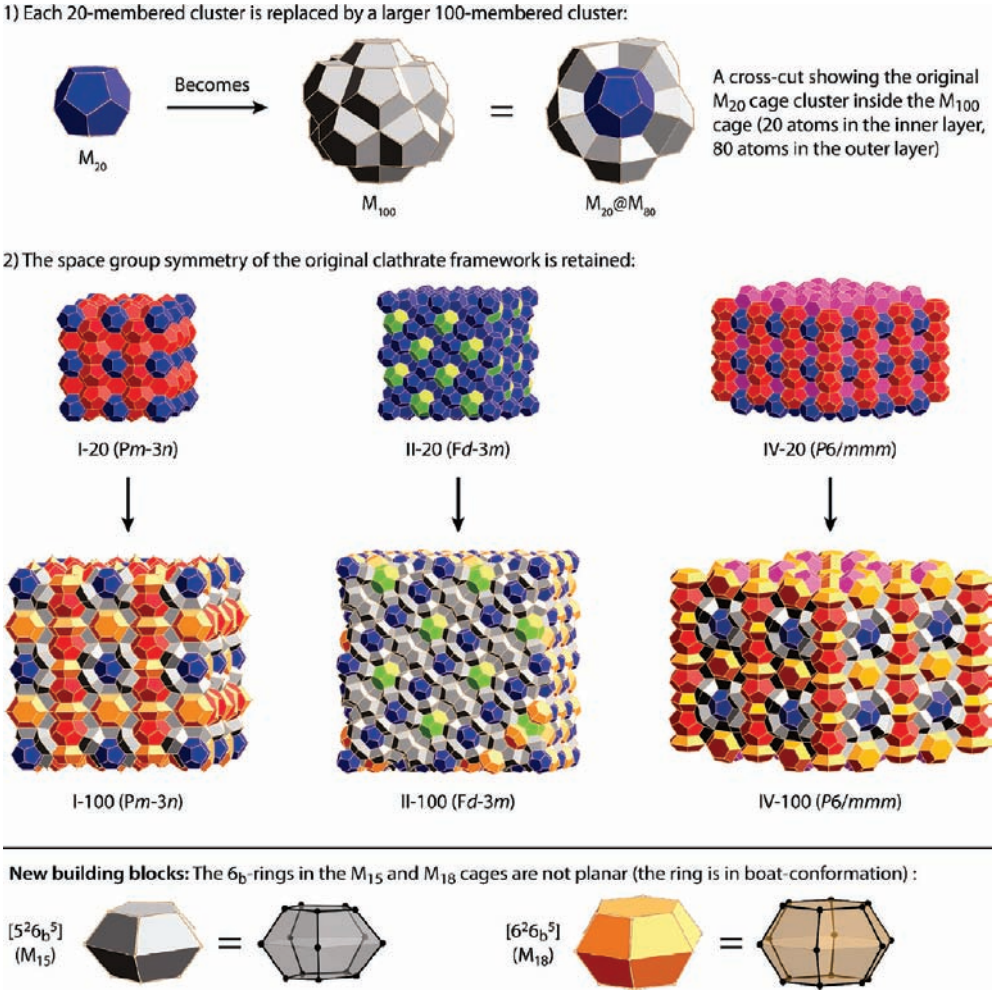

Figure 5. Structural principles of the studied extended clathrate frameworks based on larger icosahedral building blocks (I_h-clathrates).

larger icosahedral building blocks such as I−100 and II−100 (vide infra), would result in very complex clathrate frameworks.

3. Extended Clathrate Frameworks Based on Larger Icosahedral Building Blocks. As illustrated by the structural principles of the intergrowth clathrates, the basic clathrate frameworks can be used as a starting point for deriving more-complex tetracoordinated networks. Benedek et al. have investigated three structural series of hollow carbon structures, where the first members of the series are basic clathrate frameworks I, II, and IV.[30] Related topologies have also been discussed in the context of icosahedral tetracoordinated quasicrystals.[47] The frameworks derived by Benedek et al. can also be considered from another

(47) Peters, J.; Trebin, H.-R. *Phys. Rev. B* **1991**, *43*, 1820–1823.

Table 3. Guest−Vertex Distances Used in the Evaluation of the Polyhedral Cavities

cage	vertices (atoms)	Guest−Vertex Distance (Å)[a]			
		C	Si	Ge	Sn
$[5^{12}]$	20	2.09	3.21	3.35	3.84
$[5^{12}6^2]$	24	2.27	3.46	3.61	4.14
$[5^{12}6^3]$	26	2.46	3.74	3.90	4.48
$[5^{12}6^4]$	28	2.54	3.88	4.06	4.65
$[4^3 5^9 6^2 7^3]$	30	2.55	3.90	4.09	4.69
$[4^4 5^4]$	12	1.63	2.48	2.60	2.97
$[4^6 6^8]$	24	2.44	3.76	3.95	4.53
$[3^3 4^3]$	8	1.25	1.88	1.98	2.26
$[3^3 4^3 5^9]$	20 (+ 3)	2.07	3.18	3.33	3.83
$[4^3 5^6 6^3]$	20	2.02	3.09	3.24	3.72
$[5^{12}6^8]$	36	2.76	4.23	4.41	5.05
$[6^2 6_b^5]$	18	2.03	3.05	3.22	3.65
$[5^2 6_b^5]$	15	1.70	2.73	2.82	3.27

[a] Shortest distance between the centerpoint of the cage and the vertices of the cage, averaged over all clathrate frameworks containing the cage type.

Table 4. Atomic Radii Used in the Evaluation of the Polyhedral Cavities

atom	Atomic Radii (Å)		
	r(vdW)[a]	r(covalent)[b]	r(ionic)[c]
C	1.70	0.75	
Si	2.10	1.16	
Ge	2.11	1.21	
Sn	2.17	1.40	
Li	1.81	1.33	0.76
Na	2.27	1.55	1.02
K	2.75	1.96	1.38
Rb	3.03	2.10	1.52
Cs	3.43	2.32	1.67
Be	1.53	1.02	0.45
Mg	1.73	1.39	0.72
Ca	2.31	1.71	1.00
Sr	2.49	1.85	1.18
Ba	2.68	1.96	1.35
F	1.47	0.64	1.33
Cl	1.75	0.99	1.81
Br	1.83	1.14	1.96
I	1.98	1.33	2.20

[a] van der Waals radius. (See ref 50.) [b] Single-bond covalent radius. (See ref 51.) [c] Shannon ionic radius (coordination number VI). (See ref 52.)

point of view by considering the extended frameworks to be composed of larger building blocks, instead of the simple polyhedral cages. Our approach to the structures suggested by Benedek et al. was to consider them to be composed of the recently investigated icosahedral diamondoid-like structures of Group 14 elements.[31] The structural principles of the extended clathrate frameworks based on larger icosahedral building blocks (I_h-clathrates) are illustrated in Figure 5. In addition to the I_h-clathrates based on basic frameworks I, II, and IV, we also investigated an H−100 structure based on basic clathrate framework H. However, this structure turned out to be relatively strained ($\Delta E = 0.19$ eV/atom for silicon) and will not be discussed in detail. In fact, the concept of replacing $[5^{12}]$ cages with larger icosahedral building blocks also could be extended to other frameworks with $[5^{12}]$ cages. For example, I_h-clathrates of basic frameworks V and 4H−II could be derived in similar fashion to that of structurally related clathrate II, resulting in different polytypes of the I_h-clathrate II. Basic framework III also contains $[5^{12}]$ cages, but the relatively complex structure of the frameworks would lead to even more-complex I_h-clathrates, which will not be discussed here.

The relative energies, band gaps, and densities of the I_h-clathrate frameworks for all studied Group 14 elements are listed in Table 2 and illustrated in Figure 3. In the case of carbon, the I_h-clathrate frameworks are fairly strained, but for all other elements they are much more reasonable. In particular for silicon, the I_h-clathrates I−100, II−100, and IV−100 are energetically very close to their respective basic clathrate frameworks (differences are 0.01−0.02 eV/atom). The densities of the I_h-clathrates I−100, II−100, and IV−100 increase toward the dense α-structure and the band gaps decrease in comparison to the basic clathrate frameworks. In general, the I_h-clathrates can also be considered as an intermediate form between the α-structure and the basic clathrates. Band structure diagrams and simulated X-ray powder patterns of the I−100, II−100, and IV−100 clathrates can be found from the Supporting Information. The I−100 and IV−100 frameworks possess direct band gaps, while the energy gap in the framework II-100 is indirect. The large and fairly complex unit cells of the I_h-clathrates could turn out to be beneficial for tuning their thermoelectric properties, which can be strongly affected by the complexity of the unit cell.[6] For example, the lattice constant a is 16.96 Å and 24.44 Å for the I−100 and II−100 silicon I_h-clathrates, respectively.

The larger I_h-clathrates composed of 280-membered clusters ($M_{20}@M_{80}@M_{180}$)[31] analogously to the I−100, II−100, and IV−100 structures were found to be slightly more strained in comparison to their smaller counterparts. In the larger structures the 280-membered clusters cannot be packed three-dimensionally without considerable elongation of some bonds, increasing the structural strain. Therefore, the I_h-clathrates based on the 100-membered cluster appear to be the most feasible targets for experimental work among the studied I_h-clathrates.

4. Considerations toward Experimentally Feasible Clathrate Compounds. Since the clathrate frameworks are normally occupied by guest atoms, it is helpful to investigate what type of guest atoms could possibly stabilize new clathrate frameworks that have not been encountered previously. Similar to the work of Rousseau et al.,[27] we have evaluated the size distribution of the polyhedral cavities for all clathrate frameworks studied here. The importance of the size distribution of the polyhedral cavities has also been discussed by Bobev and Sevov, in conjunction with their original synthesis of clathrate II structures.[48] Generally, guest-occupied clathrates are considered to comply with the principles of the Zintl concept;[3,49] that is, the guest atoms are assumed to be ionic and donate their valence electrons to the host structure (or accept electrons from the host

(48) Bobev, S.; Sevov, S. C. *J. Am. Chem. Soc.* **1999**, *121*, 3795–3796.
(49) Gatti, C.; Bertini, L.; Blake, N. P.; Iversen, B. B. *Chem.—Eur. J.* **2003**, *9*, 4556–4568.
(50) Mantina, M.; Chamberlin, A. C.; Valero, R.; Cramer, C. J.; Truhlar, D. G. *J. Phys. Chem. A* **2009**, *113*, 5806–5812.
(51) Pyykkö, P.; Atsumi, M. *Chem.—Eur. J.* **2003**, *15*, 186–197.
(52) (a) Shannon, R. D. *Acta Crystallogr., Sect. A: Cryst. Phys., Diffr., Theor. Gen. Crystallogr.* **1976**, *32*, 155–169. (b) http://abulafia.mt.ic.ac.uk/shannon/ptable.php.

Table 5. Summary of the Polyhedral Cavities in the Studied Clathrate Frameworks

		Possible Cationic and Anionic Guests (See Text for Detailed Explanation)			
clathrate	cage (position)	C	Si	Ge	Sn
I	$[5^{12}]_2$ (0,0,0)	Be	Na, K; Ca, Sr, Ba; Cl, Br	Na, K, Rb; Ca, Sr, Ba; Cl, Br, I	K, Rb, Cs; Sr, Ba; Br, I
	$[5^{12}6^2]_6$ ($^1/_2$,0,$^1/_4$)	Li; Be, Mg; F	K, Rb, Cs; Ca, Sr, Ba; Cl, Br, I	K, Rb, Cs; Sr, Ba; Br, I	Rb, Cs; I
II	$[5^{12}]_{16}$ (0,0,0)	Be	Na, K; Ca, Sr, Ba; Cl, Br	Na, K, Rb; Ca, Sr, Ba; Cl, Br, I	K, Rb, Cs; Sr, Ba; Br, I
	$[5^{12}6^4]_8$ ($^3/_8$,$^3/_8$,$^3/_8$)	Li, Na; Mg, Ca; F, Cl	Rb, Cs; I	Rb, Cs	
III	$[5^{12}]_{10}$ (0,0,$^1/_2$); (0.750,0.566,0)	Be	Na, K; Ca, Sr, Ba; Cl, Br	Na, K, Rb; Ca, Sr, Ba; Cl, Br, I	K, Rb, Cs; Sr, Ba; Br, I
	$[5^{12}6^2]_{16}$ (0.178,0.178,0.243); (0.373,0.97,0)	Li; Be, Mg; F	K, Rb, Cs; Ca, Sr, Ba; Cl, Br, I	K, Rb, Cs; Sr, Ba; Br, I	Rb, Cs; I
	$[5^{12}6^3]_4$ (0.895,0.105,0)	Li, Na; Mg, F	K, Rb, Cs; Ba; Br, I	K, Rb, Cs; I	Cs
IV	$[5^{12}]_3$ ($^1/_2$,0,$^1/_2$)	Be	Na, K; Ca, Sr, Ba; Cl, Br	Na, K, Rb; Ca, Sr, Ba; Cl, Br, I	K, Rb, Cs; Sr, Ba; Br, I
	$[5^{12}6^2]_2$ (0,0,$^1/_4$)	Li; Be, Mg; F	K, Rb, Cs; Ca, Sr, Ba; Cl, Br, I	K, Rb, Cs; Sr, Ba; Br, I	Rb, Cs; I
	$[5^{12}6^3]_2$ ($^1/_3$,$^2/_3$,0)	Li, Na; Mg, F	K, Rb, Cs; Ba; Br, I	K, Rb, Cs; I	Cs
V	$[5^{12}]_8$ (0,0,0); ($^1/_3$,$^1/_6$,$^1/_4$)	Be	Na, K; Ca, Sr, Ba; Cl, Br	Na, K, Rb; Ca, Sr, Ba; Cl, Br, I	K, Rb, Cs; Sr, Ba; Br, I
	$[5^{12}6^4]_4$ ($^1/_3$,$^2/_3$,0.07)	Li, Na; Mg, Ca; F, Cl	Rb, Cs; I	Rb, Cs	
VI	$[4^35^96^27^3]_{16}$ (0.19,0.19,0.19)	Li, Na; Mg, Ca; F, Cl	Rb, Cs; I	Cs	(Cs)
	$[4^45^4]_{12}$ (0.875,0,0.25)		Be	Li; Be, Mg; F	Li; Be, Mg; F
VII	$[4^66^8]_2$ (0,0,0)	Li, Na; Mg; F	K, Rb, Cs; Ba; I	Rb, Cs; I	(Cs)
VIII	$[3^43^3]_6$ ($^1/_2$,0,0)				
	$[3^43^35^9]_8$ (0.186,0.186,0.186)	Be	Na, K; Ca, Sr, Ba; Cl, Br	Na, K, Rb; Ca, Sr, Ba; Cl, Br, I	K, Rb, Cs; Sr, Ba; Br, I
IX	$[5^{12}]_8$ (0.19,0.19,0.19)	Be	Na, K; Ca, Sr, Ba; Cl, Br	Na, K, Rb; Ca, Sr, Ba; Cl, Br, I	K, Rb, Cs; Sr, Ba; Br, I
H	$[5^{12}]_3$ ($^1/_2$,0,$^1/_2$)	Be	Na, K; Ca, Sr, Ba; Cl, Br	Na, K, Rb; Ca, Sr, Ba; Cl, Br, I	K, Rb, Cs; Sr, Ba; Br, I
	$[4^35^66^3]_2$ ($^2/_3$,$^1/_3$,0)	Be	Li, Na; Mg, Ca, Sr; Cl, Br	Na, K; Ca, Sr, Ba; Cl, Br	K, Rb, Cs; Sr, Ba; Cl, Br, I
	$[5^{12}6^8]_1$ (0,0,0)	Na, K; Ca, Sr, Ba; Cl, Br	Cs		
"II−4H"	$[5^{12}]_{16}$ ($^1/_2$,$^1/_2$,0); (0.15,0.30,0.25); ($^1/_3$,$^2/_3$,$^1/_8$)	Be	Na, K; Ca, Sr, Ba; Cl, Br	Na, K, Rb; Ca, Sr, Ba; Cl, Br, I	K, Rb, Cs; Sr, Ba; Br, I
	$[5^{12}6^4]_8$ (0,0,0.1); ($^2/_3$,$^1/_3$,0.15)	Li, Na; Mg, Ca; F, Cl	Rb, Cs; I	Rb, Cs	
II+IV−b	$[5^{12}]_{21}$ (1/2,1/2,0.09); ($^1/_3$,$^2/_3$,$^1/_6$)	Be	Na, K; Ca, Sr, Ba; Cl, Br	Na, K, Rb; Ca, Sr, Ba; Cl, Br, I	K, Rb, Cs; Sr, Ba; Br, I
	$[5^{12}6^2]_6$ (0,0,0.04)	Li; Be, Mg; F	K, Rb, Cs; Ca, Sr, Ba; Cl, Br, I	K, Rb, Cs; Sr, Ba; Br, I	Rb, Cs; I
	$[5^{12}6^3]_6$ (0,0,$^1/_3$)	Li, Na; Mg, F	K, Rb, Cs; Ba; Br, I	K, Rb, Cs; I	Cs
	$[5^{12}6^4]_6$ (0,0,0.155)	Li, Na; Mg, Ca; F, Cl	Rb, Cs; I	Rb, Cs	
I-100	$[5^{12}]_2$ (0,0,0)	Be	Na, K; Ca, Sr, Ba; Cl, Br	Na, K, Rb; Ca, Sr, Ba; Cl, Br, I	K, Rb, Cs; Sr, Ba; Br, I
	$[5^{12}6^2]_6$ ($^1/_2$,0,$^1/_4$)	Li; Be, Mg; F	K, Rb, Cs; Ca, Sr, Ba; Cl, Br, I	K, Rb, Cs; Sr, Ba; Br, I	Rb, Cs; I
	$[6^26_b^5]_6$ ($^1/_2$,0,0)	Be	Li, Na; Mg, Ca, Sr; Cl, Br	Na, K; Ca, Sr, Ba; Cl, Br	K, Rb, Cs; Ca, Sr, Ba; Cl, Br, I
	$[5^26_b^5]_{48}$ (0.22,0.14,0); (0.633,0.133,$^1/_4$)		Li; Be, Mg; F	Li, Na; Be, Mg; F	Li, Na; Mg, Ca, Sr; Cl, Br
II-100	$[5^{12}]_{16}$ (0,0,0)	Be	Na, K; Ca, Sr, Ba; Cl, Br	Na, K, Rb; Ca, Sr, Ba; Cl, Br, I	K,Rb,Cs; Sr, Ba; Br, I
	$[5^{12}6^4]_8$ ($^3/_8$,$^3/_8$,$^3/_8$)	Li, Na; Mg, Ca; F, Cl	Rb, Cs; I	Rb, Cs	
	$[6^26_b^5]_{16}$ ($^1/_2$,$^1/_2$,$^1/_2$)	Be	Li, Na; Mg, Ca, Sr; Cl, Br	Na, K; Ca, Sr, Ba; Cl, Br	K,Rb,Cs; Ca, Sr, Ba; Cl, Br, I
	$[5^26_b^5]_{144}$ ($0,^1/_8,^1/_8$); (−0.17, 0.058, 0.058)		Li; Be, Mg; F	Li, Na; Be, Mg; F	Li, Na; Mg, Ca, Sr; Cl, Br
IV-100	$[5^{12}]_3$ ($^1/_2$,0,$^1/_2$)	Be	Na, K; Ca,Sr,Ba; Cl, Br	Na, K, Rb; Ca, Sr, Ba; Cl, Br, I	K, Rb, Cs; Sr, Ba; Br, I
	$[5^{12}6^2]_2$ (0,0,$^1/_4$)	Li; Be, Mg; F	K, Rb, Cs; Ca, Sr, Ba; Cl, Br, I	K, Rb, Cs; Sr, Ba; Br, I	Rb, Cs; I
	$[5^{12}6^3]_2$ ($^1/_3$,$^2/_3$,0)	Li, Na; Mg, F	K, Rb, Cs; Ba; Br, I	K, Rb, Cs; I	Cs
	$[6^26_b^5]_5$ (0,0,0); (0,0,$^1/_2$)	Be	Li, Na; Mg, Ca, Sr; Cl, Br	Na, K; Ca, Sr, Ba; Cl, Br	K, Rb, Cs; Ca, Sr, Ba; Cl, Br, I
	$[5^26_b^5]_{36}$ (0.28,0.28,0.38); (0.34,0.17,0.13); (0.425,0.85,0.75)		Li; Be, Mg; F	Li, Na; Be, Mg; F	Li, Na; Mg, Ca, Sr; Cl, Br

structure in the case of the inverse clathrates composed of anionic guests and a cationic framework).[1]

Structural evaluation of the feasible guest-occupied clathrates is complicated by many factors. For example, the guest atoms are often displaced from the center of the cage and they can also "rattle" inside the empty space. Furthermore, in the guest-occupied clathrates, the structural characteristics of the framework are also usually modified because of framework heteroatoms such as Group 13 atoms. The structural characteristics of host−guest compounds have been previously evaluated by taking the average distance between the cage center and the cage vertices, subtracting the van der Waals radius of the framework atoms from this value, and comparing the resulting value with the ionic radii of the possible cationic guests.[27] However, several polyhedral cavities of the clathrate frameworks studied here are very far from a spherical shape (for example, the 36-membered $[5^{12}6^8]$ cage in clathrate H). Therefore, we have chosen to use the shortest centerpoint−vertex distances in our analysis (see Table 3). Furthermore, using the van der Waals radius (r(vdW)) of the framework and the ionic radius of the guest atom to evaluate the space requirements of the guest atom is not always an appropriate scheme. Especially for the inverse clathrates with anionic guests, the van der Waals + ionic radius approach results in unreasonable space requirements for the guests, in comparison to the structural characteristics of the experimentally known inverse clathrates. Generally, any approach that is dependent on the van der Waals, ionic, or covalent radii is necessarily approximate. We estimated the space requirements of the guest atoms with several schemes. First, we applied the r(vdW) value of the framework atom and the ionic radius of the guest atom, which results in rather good results for many cationic guests, but also space requirements that are too large for some of the cations and all of the anions, in comparison to the experiment. Next, we applied the covalent radii of both the framework atom and the guest atom, which predictably resulted in space requirements that were too small for the guests. Based on comparisons to experimentally known polyanionic and polycationic clathrate frameworks,[1] we then decided to apply the average of the values coming from the van der Waals/ionic and covalent/covalent schemes, resulting in a scheme that allows for equivalent treatment of both cationic and anionic guests (the applied atomic radii are listed in Table 4). We have taken the rattling of the guest atoms and structural expansion of the framework into account by accepting guests that occupy 85%−105% of the available space (this criterion is slightly tighter, in comparison to the 60%−110% used by Rousseau et al.[27]).

A summary of the guest atom analysis is presented in Table 5. Although the applied scheme results in rather reasonable results, in comparison to the experimentally known structures, few experimental compositions are still missed by the present scheme. For example, according to our analysis, the Cs atom would appear to be too big for the Ge-$[5^{12}]$ cages in the germanium clathrate I framework, but the $Cs_8[Ga_8Ge_{38}]$ clathrate is actually experimentally known.[1] This is reasonable, considering the complex structural characteristics of realistic guest-occupied clathrates and the approximate nature of the present analysis. Therefore, the volume-based suggestions in Table 5 should be considered only as starting points for more-detailed analyses of new, Zintl-type clathrate structures with theoretical or experimental methods. Possible further approaches include the tight-binding screening methods used by Rousseau et al.[27] and automated, high-throughput screening of Zintl-type clathrate compositions with first-principles methods.

Conclusions

We have investigated various clathrate frameworks composed of the Group 14 elements carbon, silicon, germanium, and tin. A systematic investigation of the clathrate frameworks with quantum chemical methods showed the clathrate II framework to be the energetically most favorable for all elements, in agreement with the previous experimental and theoretical results. However, the hexagonal polytypes of clathrate II (clathrates V and II−4H) were found to be practically as stable as clathrate II, suggesting that detailed investigation of the clathrate II polytypism could reveal interesting new structural characteristics within the semiconducting clathrates. The extended clathrate frameworks based of larger icosahedral building blocks possess very large and complex unit cells and guest-occupied realistic compositions, based on the I_h-clathrate frameworks, might possess attractive thermoelectric properties. Several of the studied clathrate frameworks possess direct and wide band gaps in the case of silicon, which is interesting, from the point of view of optoelectronic applications. The present comprehensive evaluation of the structural principles of the clathrate frameworks is a necessary step toward systematic studies of realistic guest-occupied clathrate compositions. Forthcoming studies on more-complex clathrate compositions are expected to be helpful in the preparation of new materials for improving energy efficiency through thermoelectric and optoelectronic applications.

Acknowledgment. We gratefully acknowledge financial support from the Academy of Finland, Finnish Funding Agency for Technology and Innovation, and European Union/European Regional Development Fund (through Grant No. 70026/08). Ville Härkönen is acknowledged for providing the data for the polyhedral constituent cages.

Supporting Information Available: Additional computational details, supplementary figures and tables, and unit-cell coordinates of the studied structures. This material is available free of charge via the Internet at http://pubs.acs.org.